Environ. Sci. Technol. **1998**, *32,* 1994−2003

Nitrogen Dioxide Absorption and Sulfite Oxidation in Aqueous Sulfite

CHEN H. SHEN AND GARY T. ROCHELLE*
Department of Chemical Engineering, The University of Texas at Austin, Austin, Texas 78712-1062

Removal of NO from flue gas may be achieved by its oxidation to NO_2 followed by absorption in sulfite solution in existing scrubbers for desulfurization. Rates of NO_2 absorption and sulfite oxidation were measured in a highly characterized stirred-cell contactor. The results were interpreted by the theory of mass transfer with fast reaction in the boundary layer. The reactions between NO_2 and sulfite (SO_3^{2-}), bisulfite (HSO_3^-), and thiosulfate ($S_2O_3^{2-}$) were first order in NO_2 concentration, and their respective rate constants at 55 °C were 11.2×10^5, 2.8×10^4, and 5.4×10^3 M^{-1} s^{-1}. The NO_2 hydrolysis reaction was second order in NO_2 concentration, with a rate constant of 1.6×10^7 M^{-1} s^{-1} at 55 °C. NO_2 absorption initiates sulfite oxidation in the presence of oxygen, and this study quantified the effect of sulfite and oxygen concentration, the rate of NO_2 absorption, and the presence of thiosulfate and gas-phase SO_2 on the rate of sulfite oxidation. With typical conditions for limestone slurry, 10 mM total dissolved S(IV) and pH 4−5, the estimated NO_2 removal was less than 50%. Therefore, an acceptable level of NO_2 removal by a conventional limestone slurry scrubber is not probable. However, NO_2 absorption is feasible in sodium sulfite inhibited by thiosulfate. NO_2 may also be an effective catalyst for sulfite oxidation in limestone slurry scrubbing.

Introduction

Limestone ($CaCO_3$) slurry scrubbing and lime (CaO) spray drying are state-of-the-art technologies for flue gas desulfurization. These systems do not remove NO because of its limited solubility and reactivity. However, NO_2 is reactive with sulfite solutions and will be removed to a significant extent by these systems. NO can be converted to NO_2 by the addition of methanol at >400 °C (*1*) or by the addition of ozone (*2, 3*) or hydrogen peroxide (*4*). Therefore, it may be feasible to achieve simultaneous SO_2 and NO_x removal by the combination of NO oxidation and conventional scrubbing of SO_2. In a typical limestone slurry scrubbing operation, dissolved sulfite is oxidized to sulfate by sparging air into the slurry hold tank. Since NO_2 absorption is shown to initiate sulfite oxidation, another possible application is to reduce oxidation air stoichiometry or to reduce the depth of the hold tank by injecting small amounts of NO_2 into the oxidation air.

NO_2 absorption occurs with simultaneous mass transfer and fast reaction. Although previous investigators have studied NO_2 reaction with sulfite, these studies were usually performed under conditions far from that of a limestone slurry scrubber. Takeuchi et al. (*5*) measured NO_2 absorption into aqueous sodium sulfite and bisulfite solutions, both in a gas liquid contactor and a spray column, and they have reported the reaction rate constant for the above reaction at 25 °C. They have studied the effect of sulfite concentration, gas-phase NO_2 partial pressure, and agitation on the rate of NO_2 absorption. They have investigated the effect of temperature between 10 and 25 °C. In another study, Takeuchi et al. (*6*) performed simultaneous absorption of SO_2 and NO_2 in aqueous solutions of NaOH and Na_2SO_3. Pigford et al. (*7*) studied the absorption of NO_2 into water, sulfuric acid, NaOH, and alkaline Na_2SO_3 solutions in a wetted sphere absorber. Their results show that the dimer form of NO_2 (N_2O_4) is the actual species being absorbed, and they have proposed a reaction mechanism to account for this observation.

NO_2 reacts with sulfite through a free radical mechanism (*8*), with the net result being that every mole of NO_2 absorbed can lead to the oxidation of 4 or more moles of sulfite in the presence of oxygen. Furthermore, it has been shown that the rate of sulfite oxidation is strongly affected by the presence of NO_2, especially when O_2 is also present in the gas phase.

There are several different objectives for this study. First, it seeks to expand our understanding of the reaction mechanism by measuring and reporting kinetic rate constants at both 25 and 55 °C. Second, this study covered a much wider range of sulfite and NO_2 concentration than any previous researchers, in particular the additional presence of SO_2 and O_2 in the gas phase and thiosulfate in the solution. Third, it develops a model to account for sulfite oxidation in the presence of NO_2, supported by actual measurements of oxidation rates. Finally, this paper attempts to predict the performance of a typical limestone slurry scrubber in removing NO_2 and proposes other possible applications of our results.

Experimental Method

All experiments were performed in a stirred cell contactor with separately agitated gas and liquid. The gas/liquid contact area was 81 cm^2. Details on the apparatus and experimental methods are same as those for NO_2 absorption in sulfide solutions (*9, 10*). This same reactor was used for SO_2 absorption in $Ca(OH)_2$ slurries (*11*).

The stirred-cell contactor was operated either continuously or in batch mode. When operating in the batch mode, the solution was fed into the reactor before each experiment and was withdrawn after each run. Nothing was added or withdrawn during the course of the experiment. While this mode of operation had the advantage of simplicity, the sulfite concentration in the solution as well as the solution pH was continuously decreasing during the course of a run, which was undesirable for most of our studies. Therefore, the majority of our experiments were performed with continuous operation.

When operating in a continuous mode, a solution containing Na_2SO_3, Na_2SO_4, and other additives such as succinic acid and sodium thiosulfate was freshly prepared and fed into the contactor. Succinic acid was added to a number of experiments to buffer the pH at the gas/liquid interface. Succinic acid is similar in buffer function to glutaric and adipic acids, common buffer additives for limestone slurry scrubbing. Sodium thiosulfate was used as an inhibitor of sulfite oxidation. The pH of the solution was adjusted by adding NaOH. Between 100 and 300 mM Na_2SO_4 was used to keep a constant ionic strength for all the runs. Once the run began, a mixture of Na_2SO_3/$NaHSO_3$/NaOH of predetermined concentration was periodically fed into the contactor for the purpose of maintaining a constant solution pH

* Address correspondence to this author. Fax: (512)471-7060; e-mail: rochelle@che.utexas.edu.

S0013-936X(97)00466-5 CCC: $15.00
Published on Web 05/27/1998

and total S(IV) concentration, and the same volume of solution was withdrawn from the contactor at the same time for solution analysis. Important variables such as the pressure inside the contactor, the temperature, the solution pH, and the liquid and gas agitation rates were monitored and controlled.

The rates of sulfite oxidation and oxygen absorption were determined by iodimetric titration of the samples to get total S(IV) and thiosulfate in the solution. When only SO_3^{2-}/HSO_3^- was present, the concentration of total S(IV) was determined by a one-step titration (*12*). An excess amount of iodine of known concentration was introduced into the sample, and then the sample was back-titrated with a standard thiosulfate solution until the color disappeared. When both SO_3^{2-} and $S_2O_3^{2-}$ were present, the concentration of individual S(IV) and $S_2O_3^{2-}$ was determined by iodometric titration with and without formaldehyde (*13*). This procedure tracks only disappearance of S(IV) and assumes that oxidants and other interfering species such as HSO_5^- are present at concentrations much less than the S(IV).

Chemistry and Theory

The actual mechanism of the reaction between NO_2 and aqueous sulfite solution is rather complex. Nash (*14*) proposed that such a reaction was likely to involve charge transfer that might lead to a free radical chain mechanism. Three irreversible parallel reactions may occur in the boundary layer and enhance NO_2 absorption. These reactions are as follows:

$$NO_2 + SO_3^{2-} \rightarrow NO_2^- + SO_3^{\bullet -}$$
$$r_{SO_3^{2-}} = k_{2,SO_3^{2-}}[SO_3^{2-}]_i[NO_2]_i \quad (1)$$

$$NO_2 + HSO_3^- \rightarrow NO_2^- + HSO_3^{\bullet}$$
$$r_{HSO_3^-} = k_{2,HSO_3^-}[HSO_3^-]_i[NO_2]_i \quad (2)$$

$$2NO_2 + H_2O \rightarrow HNO_2 + HNO_3$$
$$r_{H_2O} = k_{2,H_2O}[NO_2]_i^2 \quad (3)$$

where $[SO_3^{2-}]_i$, $[HSO_3^-]_i$, and $[NO_2]_i$ are the interfacial concentrations of sulfite, bisulfite, and NO_2, respectively.

When thiosulfate is added to the solution, it can also react with NO_2 by the following reaction:

$$NO_2 + S_2O_3^{2-} \rightarrow NO_2^- + S_2O_3^{\bullet -}$$
$$r_{S_2O_3^{2-}} = k_{2,S_2O_3^{2-}}[S_2O_3^{2-}]_i[NO_2]_i \quad (4)$$

When SO_2 is added to the gas phase, the following equilibrium reaction takes place:

$$SO_2 + SO_3^{2-} + H_2O \leftrightarrow 2HSO_3^- \quad (5)$$

which has the net effect of increasing the concentration of total S(IV) in the solution while reducing the solution pH.

When absorbing NO_2 into sulfite solutions, assuming fast reactions and using the reaction kinetics at the gas/liquid interface, the flux of NO_2 (N_{NO_2}) should be given approximately by (*15, 16*)

$$N_{NO_2} = \frac{P_{NO_{2,i}}}{H_{NO_2}}\left[D_{NO_2}\left(k_{2,SO_3^{2-}}[SO_3^{2-}]_i + k_{2,HSO_3^-}[HSO_3^-]_i + \frac{2}{3}\frac{k_{2,H_2O}P_{NO_{2,i}}}{H_{NO_2}} + k_{2,S_2O_3^{2-}}[S_2O_3^{2-}]_i\right)\right]^{1/2} \quad (6)$$

Rearranging eq 6 to a linear form gives

$$\frac{R_g^2 H_{NO_2}^2}{D_{NO_2}} = k_{2,SO_3^{2-}}[SO_3^{2-}]_i + k_{2,HSO_3^-}[HSO_3^-]_i + \frac{2}{3}\frac{k_{2,H_2O}P_{NO_{2,i}}}{H_{NO_2}} + k_{2,S_2O_3^{2-}}[S_2O_3^{2-}]_i \quad (7)$$

where R_g is a normalized rate of absorption given by the following:

$$R_g = \frac{N_{NO_2}}{P_{NO_{2,i}}} \quad (8)$$

P_{NO2i} is the interfacial partial pressure of NO_2 and is given by

$$P_{NO_{2,i}} = P_{NO_{2,b}} - \frac{N_{NO_2}}{k_g} \quad (9)$$

where $P_{NO_2,b}$ is the measured bulk partial pressure of NO_2, and k_g is the gas-phase mass transfer coefficient, measured by SO_2 absorption in NaOH solution (*9*):

$$k_g A\ [\text{mol s}^{-1}\ \text{bar}^{-1}] = 4.95 \times 10^{-5}\ (\text{gas agitation speed})^{0.76} \quad (10)$$

At 650 rpm, $k_g = 1.0 \times 10^{-4}$ mol cm^{-2} s^{-1} atm^{-1}. In the absence of gas film resistance, R_g is identical to K_g, the overall gas-phase mass transfer coefficient. The diffusion coefficient of dissolved NO_2 (D_{NO_2}) was taken to be 3.28×10^{-5} cm^2 s^{-1} at 55 °C (*17*). The Henry's constant for NO_2 (H_{NO_2}) was taken to be 4.76×10^4 cm^{-3} atm^{-1} mol^{-1} at 55 °C (*18*).

Oblath et al. (*19, 20*) studied the reactions between NO_2 and sulfite, and they found that the product of this reaction was a family of nitrososulfonates, including $HON(SO_3)_2^{2-}$, $HONHSO_3^-$, $HN(SO_3)_2^{2-}$, and $N(SO_3)_2^{2-}$. They found that the rates of these reactions are too small for them to occur to any significant extent in the boundary layer, so the formation of these nitrogen−sulfur compounds is expected to occur in the bulk solution.

In the presence of oxygen, the free radicals produced by NO_2 reaction with sulfite and bisulfite were found to initiate sulfite oxidation in a chain mechanism (*8, 21*). These reactions are expected to occur in the mass transfer boundary layer. One direct consequence of this mechanism is the depletion of sulfite in the liquid boundary. For every mole of NO_2 absorbed, several moles of SO_3^{2-} can be consumed if oxygen is present. Therefore, when oxygen is present, the rate of NO_2 absorption is expected to be lower. Takeuchi et al. (*22*) observed that the absorption rate of NO_2 into sodium sulfite solution was about 40% lower in air rather than nitrogen. We believe that this difference was caused by the oxidation of sulfite by dissolved oxygen, and we have quantified this effect by accounting for sulfite depetion at the gas/liquid interface. The effect could also be caused by regeneration of NO_2 from nitrite in the presence of oxygen, but our results did not require this additional mechanism.

Owens (*23*) studied sulfite oxidation and thiosulfate degradation in FGD systems. He concluded that thiosulfate ($S_2O_3^{2-}$) was a strong inhibitor of sulfite oxidation. He suggested that thiosulfate could act as a free radical scavenger and thus was able to terminate the sulfite oxidation mechanism. In a system where NO_2 was absorbed into a sulfite

solution, thiosulfate could reduce the rate of sulfite oxidation by providing an alternative route for free radical termination:

$$R^{\bullet} + S_2O_3^{2-} \rightarrow R + S_2O_3^{\bullet -} \quad (11)$$

$$S_2O_3^{\bullet -} + S_2O_3^{\bullet -} \rightarrow S_4O_6^{2-} \quad (12)$$

The rate of sulfite oxidation (N_{ox}, mol cm^{-2} s^{-1}) was calculated from experimental data with the following material balance:

$$N_{ox} = \frac{V([S(IV)]_o - [S(IV)]_f) + V_{tit}[S(IV)]_{tit}}{A\Delta t} + N_{SO_2} \quad (13)$$

where $[S(IV)]_o$ and $[S(IV)]_f$ are the initial and final concentration of total S(IV) measured by iodimetric titration, respectively; Δt is the time interval; and V and A are the volume of the solution and the gas−liquid contacting area, respectively. The $V_{tit}[S(IV)]_{tit}$ term takes into account the amount of S(IV) being fed into the contactor over the course of one experiment, while the last term accounts for the additional sulfite formed by the absorption of SO_2.

To regress the four reaction rate constants from eq 7, it is necessary to have accurate estimates of $[SO_3^{2-}]_i$, $[HSO_3^-]_i$, and $[NO_2]_i$, the interfacial concentrations of sulfite, bisulfite, and NO_2. This was done by using the Bechtel-Modified Radian Equilibrium Program (BMREP) (*24*), an equilibrium program capable of calculating the concentrations of all major species in the SO_3^{2-} system, given the ionic strength, pH, total [S(IV)] and [S(VI)], total $[Na^+]$ and other metal ions present, and the concentration of buffer. To calculate $[SO_3^{2-}]_i$ and $[HSO_3^-]_i$, the bulk solution $[SO_3^{2-}]$ and $[HSO_3^-]$ were first calculated by the equilibrium program, and then by using the experimentally measured rate of sulfite oxidation calculated in eq 13, the [S(IV)] at the interface was estimated from the following equation:

$$[S(IV)]_i = [S(IV)]_b - \frac{N_{ox}}{k_l^{\circ}{}_{S(IV)}} \quad (14)$$

This relationship assumes that all of the sulfite oxidation occurs near the gas/liquid interface. The equilibrium program was used again at interfacial condition to obtain the interfacial concentrations of sulfite and bisulfite. In the above equation, $k_l^{\circ}{}_{S(IV)}$ is the liquid-phase mass transfer coefficient of S(IV) species, which is taken to be the same as $k_l^{\circ}{}_{SO_3^{2-}}$. The liquid film mass transfer coefficient was measured by absorption of SO_2 in HCl solution (*9*). The value of $k_l^{\circ}{}_{SO_3^{2-}}$ is given as a function of liquid agitation:

$$k_l^{\circ}{}_{SO_3^{2-}}\,[m/s] = 6.13 \times 10^{-7}(\text{liquid agitation speed})^{0.65} \quad (15)$$

A parameter estimation program was then used to regress the four rate constants in the linear form of eq 7 for any given set of experiments.

Results and Discussion

Results of Continuous Experiments. *NO_2 Absorption.* The results of the continuous experiments are given in Tables 1 and 2. Table 1 summarizes the results of continuous experiments in the absence of additives, while Table 2 gives the results with various liquid- and gas-phase additives. A series of experiments with 15% O_2 were regressed to obtain the rate constants from eq 7. We did not include experiments without oxygen, without buffer, with SO_2, or with other unusual conditions or poor data quality. Table 3 compares the regressed values of rate constants at 55 °C with those measured by Takeuchi at 25 °C. Table 4 gives selected results with other salts and additives.

Clifton et al. (*25*) report measured values of $k_{2,SO_3^{2-}}$ an order of magnitude larger (1.2−2.9 × 10^7 M^{-1} s^{-1} at pH 5.3−13 and ambient temperature) than extracted from our absorption experiments. Furthermore, their rates did not decrease with pH as much as observed in our stirred-cell contactor. Their experiments were performed by pulsed radiolysis in the presence of 10 mM nitrite, 0.5−2 mM sulfite, and 5 μM NO_2. The time scale of Clifton's kinetic measurements was 10^{-4} s, as compared to 1 s in the stirred-cell contactor. The discrepancy in apparent rates suggests that the reaction mechanism may be more complicated than the simple mechanism successfully used to model the stirred cell results. It is possible that Clifton was measuring the formation of an addition complex such as $O_2NOSO_2^{2-}$. If such a complex were formed quickly and reversibly at an equilibrium concentration less than 10 times the NO_2 concentration, it would not affect the interpretation of the absorption results. The one detailed experiment reported by Clifton shows an exponential decay of NO_2 absorbance to a value significantly above the baseline, suggesting that their reaction with sulfite approaches an equilibrium conversion of about 90% in less than 10^{-4} s.

The relatively large confidence interval for k_{2,H_2O} is due to the small number of pure water absorption experiments as well as the relatively minor contribution of the water reaction to the overall rate of NO_2 absorption in most of the experiments. However, the use of the full model in eq 7 is justified, since in most of the experiments, the reaction between NO_2 and HSO_3^- and $S_2O_3^{2-}$ contributed significantly to the overall rate of NO_2 absorption.

The model predicts the effects of O_2, thiosulfate, and SO_2 on the rate of NO_2 absorption. In Tables 1 and 2, we used these fitted rate constants to calculate a rate of absorption for all the other experiments in Tables 1 and 2. The comparison is given as the ratio of the estimated and measured values of the normalized flux, R_g. All of the data fall within 10−30% of the model.

When O_2 is present in the gas phase, sulfite oxidation is enhanced, and the result is lower SO_3^{2-} at the gas/liquid interface. Once this lower $[SO_3^{2-}]_i$ is accounted for by the model, these data points are represented quite well.

The effect of SO_2 depends on the buffer concentration. For every mole of SO_2 absorbed, 1 mol of SO_3^{2-} is consumed, and 2 mol of HSO_3^- is formed. The net effect of SO_2 absorption is an increase in total S(IV) concentration and a drop in pH at the interface. When a buffer such as succinate is present in the liquid phase, the change in pH is minimized, and the absorption of SO_2 leads to an increase in the rate of NO_2 absorption by adding to the total amount of S(IV). On the other hand, when no buffer is present, SO_2 absorption tends to inhibit the rate of NO_2 absorption by reducing the pH at the liquid boundary and reducing the fraction of S(IV) present as sulfite.

Figure 1 gives the normalized rate of NO_2 absorption (R_g) calculated by eq 7 as a function of pH and dissolved S(IV). The rate of NO_2 absorption increases with increasing S(IV) and pH, as both conditions lead to higher concentrations of SO_3^{2-} in the solution. Because the experimental data points include ranges of S(IV), they do not fall on the calculated lines at exact values of S(IV).

Table 4 gives selected results with significant concentrations of major ions expected in limestone slurry scrubbing. The rates of NO_2 absorption and sulfite disappearance were estimated from eq 6. Equation 6 overpredicts NO_2 absorption rates in the experiments with 600 mM chloride (Na^+, Ca^{2+}, and Mg^{2+}) by 60%. It is possible that the dichloride radical

TABLE 1. Summary of Continuous Results, No Additive, 55 °C

pH	$[S(IV)]_b$ (mM)	$[SO_3^{2-}]_b$ (mM)	$[SO_3^{2-}]_i$ (mM)	$P_{NO_2,i} \times 10^6$ (atm)	O_2 (%)	$R_{g,exp} \times 10^6$ (mol/(cm^2 s atm))	$R_{g,mod}/R_{g,exp}$ [c]	$N_{ox} \times 10^8$ (mol/(cm^2 s))	$N_{ox,mod}/N_{ox,exp}$ [d]	Na_2SO_4 (M)	succinate (M)
4.5	40.9	0.63	0.54	79.8	15	4.8[a]	1.02	2.31[b]	0.86	0.25	0.1
5.0	0	0	0	106	15	0.98[a]	1.01			0.3	0.1
5.0	0	0	0	129	15	1.1[a]	1.10			0.3	0.1
5.0	6.77	0.32	0.26	92	15	2.7[a]	0.99	0.49[b]	0.92	0.29	0.1
5.0	7.41	0.16	0	136	15	2.5[a]	0.97	0.30[b]	1.02	0.29	0.3
5.0	38.0	2.0	1.56	65	15	6.1[a]	0.98	3.47[b]	1.11	0.25	0.3
5.0	38.8	1.5	1.2	94	15	5.1[a]	0.98	2.97[b]	0.95	0.25	0.1
5.0	39.6	1.49	1.38	80	15	3.1[a]	1.03	2.74[b]	1.05	0.25	0.3
5.1	1.43	0.036	0	136	15	2.5[a]	0.98	0.30		0.3	0.1
5.5	14.8	0.98	0.63	156	15	3.9[a]	0.99	1.23[b]	0.75	0.29	0.1
6.0	73.4	14.9	2.88	172	15	15.2[a]	1.00	2.96	0.10	0.2	0.1
4.5	42.5	0.64	0.56	82.4	0	4.4	0.95	0.26		0.25	0.1
5.0	16.2	0.34	0.27	216	0	2.7	1.12	0.28		0.29	0.1
5.0	42.2	1.9	1.61	88	0	6.1	0.81	0.25		0.25	0.1
5.1	1.74	0.045	0	133	0	2.8	1.09	0.27		0.3	0.1
5.0	13.2	0.27	0.11	227	0	2.2	0.98	0.30		0.09	
5.1	45.3	2.5	1.08	79	0	6.3	2.06	0.24		0.25	
5.5	10	0.68	0.29	80	0	5.3	0.74	0.24		0.096	
5.0	0	0	0	131	15	0.89	0.82				
5.0[e]	10	0.2	0	38	15	1.0	0.68	0.60	0.72	0.096	
5.0[e]	10	0.22	0	290	15	2.2	0.75	0.73		0.096	
5.0[e]	10	0.35	0	42	15	0.9	0.61	0.53	0.58	0.096	
5.1	43.4	2.1	0.32	85	15	5.3	1.28	3.22[b]	1.15	0.25	
5.4	10.8	0.9	0	500	15	3.3	1.64	0.94		0.096	
5.5	10	0.54	0	75	15	2.0	0.61	0.98	0.45	0.096	
5.5	10	0.63	0	97	15	1.9	0.68	1.82[b]	1.08	0.096	
5.5	10	0.59	0	105	15	1.6	0.52	1.30	0.77	0.096	
5.5	10	0.68	0	116	15	1.3	0.59	0.66		0.096	
6.0	10	1.8	0.16	65	15	4.3	1.53	1.02	0.10	0.096	
6.0[f]	87.0	17.5	3.2	15	15	15.4	1.24	4.76	1.28	0.2	
6.0[f]	87.0	14.5	0.73	233	15	12.3	0.79	8.20	1.22	0.2	
6.0[f]	87.0	14.0	0.65	16	15	18.1	0.85	10.8	1.78	0.2	
4.9	8.32	0.31	0.14	85	15	7.5	0.39	0.68		0.29	0.1
5.7	6.76	1.304	1.05	58	15	2.1	1.35	0.62[b]	1.12	0.25	0.1
5.58	6.96	1.087	0.66	53.3	15	2.63	1.31	0.50		0.25	0.1
5.58	6.77	1.023	0.84	52.2	5	3.06	1.13	3.21	1.51	0.25	0.1
5.64	6.68	0.963	0.82	35.3	1	3.53	1.20	15.1[b]	0.99	0.25	0.1
5.52	7.73	1.016	0.78	45.8	10	5.21	0.85	2.00[b]	0.92	0.25	0.1
5.38	80.7	9.408	8.32	52.1	15	9.72	1.18	5.96[b]	1.06	0.20	0.2
5.46	46.8	6.55	5.74	69.1	15	4.70	1.86	4.16	0.87	0.25	0.15
5.48	9.887	1.29	1.04	245.1	15	3.43	1.28	1.91	0.09	0.25	0.1
5.52	42.22	6.456	4.82	350.2	15	7.28	1.21	7.43	1.30	0.25	0.15

[a] These runs were used to regress the reaction rate constants $k_{2,SO_3^{2-}}$, k_{2,HSO_3^-}, k_{2,H_2O}, and $k_{2,S_2O_3^{2-}}$ from eq 7. [b] These runs were used to regress the oxidation rate constants C_1 and C_2 from eq 16. [c] The ratio of values of the normalized NO_2 flux (R_g) calculated from eq 6 and measured values. [d] The ratio of values of the oxidation flux (N_{ox}) calculated from eq 16 to measured values. [e] N products were allowed to accumulate to 0.2 mM in the second and third run of this series. [f] N products were allowed to accumulate to 1.3 mM in the second and third run of this series.

participates in the mechanism to regenerate NO_2 and slow the net rate of NO_2 absorption.

The results with 500 mM $MgSO_4$ suggest that there is no significant effect of the cation on NO_2 absorption. The model calculation accounts for the complexing effect of Mg^{2+} by assuming that sulfite ion pairs with Ca^{2+} and Mg^{2+} are unreactive to NO_2. Previous work by Takeuchi et al. (*5*) showed that rates of NO_2 absorption in 0.1 M Na^+, K^+, and NH_4^+ varied by less than 20%. The experiments with added EDTA and Fe^{2+} had no significant effects on NO_2 absorption.

Most of the experiments reported here did not run long enough to permit the accumulation of products from sulfite oxidation or NO_2 absorption at levels that could affect the measured rates. However, in two series of experiments reported in Table 1, nitrogen products were allowed to accumulate to 0.2 and 1.3 mM (pH 5 and pH 6), respectively, by absorbing a high concentration of NO_2 for an extended period of time. The absorption rate of NO_2 was practically unaffected by the accumulation of nitrogen reaction products. The sulfite oxidation rate was unchanged at pH 5 but increased a factor of 2 at pH 6. In both series, analysis of the solutions by ion chromatography recovered practically all of the absorbed NO_2 as 21% hydroxylamine disulfonic acid, 62% amine disulfonic acid, 12% nitrate, and 5% nitrite.

Sulfite Oxidation. We found that the rate of sulfite oxidation was strongly influenced by the presence of NO_2, and there is a direct correlation between the rate of sulfite oxidation and the rate of NO_2 absorption. To quantify this effect of NO_2 absorption on sulfite oxidation, we developed a semiempirical correlation of sulfite oxidation:

$$N_{ox} = C_1\sqrt{N_{NO_2}}[O_2]_i + C_2\sqrt{N_{NO_2}}[SO_3^{2-}]_i + k_l^\circ{}_{O_2}[O_2]_i \quad (16)$$

The first term accounts for sulfite oxidation limited by O_2 in the liquid phase, the second term accounts for oxidation limited by SO_3^{2-}, and the last term accounts for physical absorption of oxygen. The liquid-phase mass transfer coefficient of O_2, $k_l^\circ{}_{O_2}$, was calculated from eq 15. The diffusivity of dissolved O_2 (D_{O_2}) was taken to be 4.79×10^{-5} cm^2 s^{-1} at 55 °C. The Henry's constant for oxygen was taken to be 60 850 atm/mol fraction from Perry's Handbook. A series of experiments was chosen from Tables 1 and 2, and a parameter estimation program was used to estimate the constants C_1 and C_2. We did not include experiments without

TABLE 2. Summary of Continuous Results, with Additives, 55 °C

pH	$[S(IV)]_b$ (mM)	$[SO_3^{2-}]_b$ (mM)	$[SO_3^{2-}]_i$ (mM)	$P_{NO_2,i} \times 10^6$ (atm)	O_2 (%)	$R_{g,exp} \times 10^6$ (mol/(cm² s atm))	$R_{g,mod}/R_{g,exp}$ [c]	$N_{ox} \times 10^8$ (mol/(cm² s))	$N_{ox,mod}/N_{ox,exp}$ [d]	Na_2SO_4 (M)	additive	succinate (M)
5.51	12.5		1.94	86.1	0	10.3	0.88			0.25	35.9 ppm SO_2	0.1
5.52	14.8		2.28	60.1	0	8.48	0.90			0.25	36.8 ppm SO_2	0.1
5.51	16.3		2.33	42.8	0	8.41	0.93			0.25	24.5 ppm SO_2	0.1
5.51	11.9		1.65	45.4	15	3.28	0.95	1.63	0.90	0.25	25.3 ppm SO_2	0.1
5.51	12.5		1.58	56.1	15	2.10	0.99	1.86	0.85	0.25	16.7 ppm SO_2	0.1
5.46	0.97		1.45	228.5	0	2.30	1.18			0.25	105.8 ppm SO_2	0.1
5.48	2.37		1.35	230.1	15	2.23	1.23	0.63	1.11	0.25	106.8 ppm SO_2	0.1
4.45	12.4	0.9	0.81	242	15	2.18	1.13	1.93	1.07	0.25	117 ppm SO_2	0.1
4.48	17.0	0.38	0.23	248	15	3.10	0.92	2.93	0.81	0.25	111 ppm SO_2	0.1
9.87	72.1	78.9	54.0	168	15	9.2	1.22	14.5	1.05	0.15		
9.78	78.9	78.9	57.9	96	15	19.0	1.02	11.8	1.21	0.15	68 ppm SO_2	
9.96	76.8	76.8	70.5	24	15	19.3	1.15	9.63	1.13	0.2		
9.91	81.1	81.1	75.2	34	15	20.0	1.14	11.6	1.24	0.2		
5.53	89.3		14.2	47.3	0	11.3	1.15				90 mM $S_2O_3^{2-}$	
5.57	81.5		13.8	49.9	15	10.3[a]	1.27	0.41[e]	1.18		90 mM $S_2O_3^{2-}$	
5.4	91		9.8	46.1	0	9.11	1.20				7.0 mM $S_2O_3^{2-}$	
5.4	82.9		8.5	46.3	15	9.15[a]	1.12	0.53[e]	1.34		7.0 mM $S_2O_3^{2-}$	
5.63[b]	0	0	0	91.2	0	2.31					88.7 mM $S_2O_3^{2-}$	
5.46[b]	0	0	0	90.3	15	2.41					87 mM $S_2O_3^{2-}$	
5.83	0	0	0	98.1	0	1.88	0.86				86.1 mM $S_2O_3^{2-}$	
6.03	0	0	0	90.6	15	2.66[a]	0.91				88.4 mM $S_2O_3^{2-}$	
6.11[b]	86.0		33.3	63.1	0	7.67					8.2 mM $S_2O_3^{2-}$	
6.14[b]	79.4		31.8	68.7	15	6.42		0.37			6.7 mM $S_2O_3^{2-}$	
7.71	98	93	85.8	17.2	15	36[a]	0.83	3.19[e]	0.81		103 mM $S_2O_3^{2-}$	
7.70	84	80	74.5	150.7	15	24[a]	1.05	2.86[e]	1.21		99.2 mM $S_2O_3^{2-}$	
7.45	103	91	82.5	21.0	15	33[a]	0.90	3.52[e]	1.28		10.2 mM $S_2O_3^{2-}$	
7.35	81	70	60	185.7	15	19[a]	1.14	4.10[e]	0.95		9.2 mM $S_2O_3^{2-}$	
7.65	9.9	8.5	7.5	15.2	15	10[a]	0.90	0.43[e]	1.00		10.3 mM $S_2O_3^{2-}$	
7.49	6.2	5.1	3.3	190.1	15	4.3[a]	1.12	0.81[e]	0.86		9.5 mM $S_2O_3^{2-}$	
7.81	10.7	10.0	9.6	17.5	15	12[a]	0.84	0.32[e]	0.78		103 mM $S_2O_3^{2-}$	
7.86	8.6	8.1	7.7	177.1	15	6.1[a]	1.24	0.46[e]	1.03		104 mM $S_2O_3^{2-}$	

[a] These runs were used to regress the reaction rate constants $k_{2,SO_3^{2-}}$, k_{2,HSO_3^-}, k_{2,H_2O}, and $k_{2,S_2O_3^{2-}}$ from eq 7. [b] $T = 25$ °C. Our model of NO_2 absorption and sulfite oxidation do not apply to these runs. [c] The ratio of values of the normalized NO_2 flux (R_g) calculated from eq 6 to measured values. [d] The ratio of values of the oxidation flux (N_{ox}) calculated from eq 16 (or eq 22 with thiosulfate) to measured values. [e] These runs were used to regress the ratio k_{ox}/k_t from eq 22, and N_{ox} is calculated using eq 22.

TABLE 3. Regressed Values of Rate Constants

reaction	reaction rate constant ($M^{-1} s^{-1}$) regressed at 55 °C	Takeuchi (*5*) at 25 °C
$k_{2,SO_3^{2-}}$	$(11.2 \pm 0.3) \times 10^5$	6.6×10^5
k_{2,HSO_3^-}	$(2.8 \pm 0.1) \times 10^4$	1.5×10^4
k_{2,H_2O}	$(1.6 \pm 1.1) \times 10^7$	7.4×10^7
$k_{2,S_2O_3^{2-}}$	$(5.4 \pm 0.6) \times 10^3$	

buffer, with SO_2, with thiosulfate, or with other unusual conditions or poor data quality. The results are as follows:

$$C_1 = (3.7 \pm 0.63) \times 10^3 \text{ cm}^2 \text{ mol}^{-1/2} \text{ s}^{-1/2}$$

$$C_2 = (0.093 \pm 0.022) \times 10^3 \text{ cm}^2 \text{ mol}^{-1/2} \text{ s}^{-1/2}$$

Tables 1 and 2 give the ratio of the predicted and measured rates of sulfite oxidation. The overall fit of the data is reasonably good, with an average absolute deviation of 35% from the experimental oxidation rates. Therefore, the rate of sulfite oxidation is proven to increase with increasing NO_2 absorption rate as well as increasing sulfite and O_2 concentration. The data that show the largest deviation from the model occurred with no buffer and relatively high NO_2 in the gas phase. Under these conditions, the depletion of SO_3^{2-} at the interface due to oxidation was extreme, and the interfacial solution pH could be significantly below the model prediction, which in turn would lead to inaccurate prediction of $[SO_3^{2-}]_i$ and the rate of sulfite oxidation by the model.

The results of a series of experiments with gas-phase SO_2 that were not used in the regression are also given in Tables 1 and 2. Previously, we have shown the effect of SO_2 on NO_2 absorption into sulfite solutions. The absorption of SO_2 into sulfite solutions leads to an increase in the interfacial S(IV) concentration, which, in the presence of a buffer, results in a higher rate of NO_2 absorption as well as sulfite oxidation. On the other hand, when no buffer is present, SO_2 absorption leads to a decrease in interfacial solution pH, which in turn reduces the concentration of SO_3^{2-} at the interface, resulting in slower rates of NO_2 absorption and sulfite oxidation.

Figure 2 gives rates of sulfite oxidation calculated from eq 16. The rate of sulfite oxidation increases with increasing sulfite concentration and NO_2 absorption. With 15% oxygen, the rate of sulfite oxidation varies from 7 to 300 times the rate of NO_2 absorption. Because the experimental data points include ranges of S(IV), they do not fall on the calculated lines at exact values of S(IV).

Table 4 includes other experiments with added chloride, Fe^{2+}, and EDTA to determine their effects on sulfite oxidation in the presence of NO_2. These experimental results are compared to the predictions of eq 16. Chloride at 600 mM reduces the rate of NO_2 absorption, but increases the rate of oxidation almost a factor of 2. Clarke and Radojevic (*26*) found that sulfite oxidation in the absence of NO_2 was enhanced with $>10^{-3}$ M chloride. The catalytic effect of chloride could result from reducing the concentration of sulfate radical, which could otherwise participate in a termination reaction:

$$SO_4^{\bullet-} + Cl^- \rightarrow SO_4^{2-} + Cl^{\bullet}$$

$$Cl^{\bullet} + Cl^- \rightarrow Cl_2^{\bullet-}$$

$$Cl_2^{\bullet-} + SO_3^{2-} \rightarrow 2Cl^- + SO_3^{\bullet-}$$

TABLE 4. Selected Continuous Experiments with Other Anions, Cations, and Metals, 55 °C, 15% O_2, 0.1 M Succinate, 0.25−0.3 M Na_2SO_4

pH	$[S(IV)]_b$ (mM)	$[SO_3^{2-}]_i$ (mM)	$P_{NO_2,i} \times 10^6$ (atm)	$R_{g,exp} \times 10^6$ (mol/(cm² s atm))	$R_{g,mod}/R_{g,exp}$	$N_{ox} \times 10^8$ (mol/(cm² s))	$N_{ox,mod}/N_{ox,exp}$	additive (mM)
5.0	38.7	2.0	74	3.8	1.58	1.60	0.48	600 NaCl
5.1	37.8	1.57	82	2.1	1.11	0.40	0.88	500 $MgSO_4$[a]
5.0	7.12	2.21	87	7.1	1.66	0.41	0.48	300 $CaCl_2$
5.0	6.0	0.22	79	1.6	1.70	0.51	0.55	300 $MgCl_2$
5.65	6.43	0.96	64	3.2	1.31	0.71	0.74	0.02 Fe^{2+}
5.61	7.15	1.05	0	0	1.15	0.30	0.67	0.026 Fe^{2+}
5.65	6.75	1.03	49.2	5.0	0.94	0.65	1.08	0.02 EDTA
5.52	7.16	0.91	0	0	0.78	0.13	1.21	0.02 EDTA
5.57	6.26	0.82	15.65	1.93	1.25	0.37	0.82	0.017 Fe^{2+}

[a] 0.3 M succinate.

TABLE 5. Summary of Batch Results, 200−1000 ppm NO_2

reagent (M)	pH	O_2 (%)	$R_g \times 10^6$ (mol/(cm² s atm))	$k_2 \times 10^{-5}$ (M^{-1} s^{-1})	T (°C)
0.085[a] Na_2SO_3	9.6	0	39.5	6.3	25
0.085[a] Na_2SO_3	9.6	0	41.3	18.7	55
0.45[a] Na_2SO_3	10.1	0	57.7	0.94	10
0.45[a] Na_2SO_3	10.1	0	73.9	1.9	15
0.45[a] Na_2SO_3	10.1	0	49.5	2.0	25
0.085[a] Na_2SO_3	9.6	15	18.2	1.1[b]	25
0.09[a] $NaHSO_3$	4.2	0	3.8	0.083	25
0.1 $Na_2S_2O_3$	8.7	0	4.7	0.079	25
0.1 Na_2SO_3 and 0.1 $Na_2S_2O_3$	9.6	0	39.0	6.0	25
0.1 Na_2SO_3 and 0.5 $Na_2S_2O_3$	9.2	0	35.6	5.1	25
0.085 Na_2S and 0.1 NaOH	12.3	0	34.6	4.7	25
0.085 Na_2S and 0.1 NaOH	12.3	15	16.8	2.5	25
0.1 Na_2S, 0.1 NaOH, and 0.5 $Na_2S_2O_3$	12.7	15	32.8	9.4	25
pure H_2O		0	3.1	271[c]	25

[a] These concentrations were estimated empirically by taking into account the oxidation of SO_3^{2-} prior to each experiment. [b] k_2 was calculated using an interfacial $[SO_3^{2-}]$, estimated by BMREP. [c] k_{2,H_2O} (see eq 6).

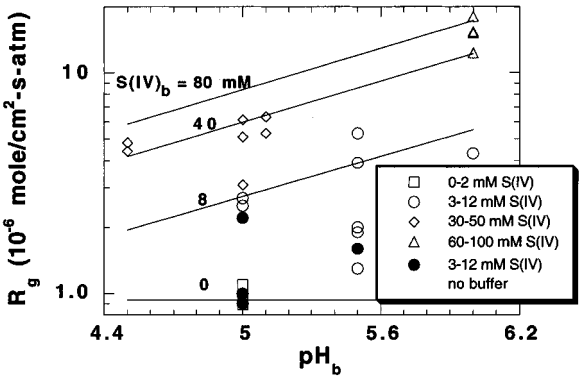

FIGURE 1. Predicted and measured rates of NO_2 absorption. Most contain succinate buffer, 55 °C, 15% O_2. $Y_{NO_2,i}$ (ppm): calculated = 100, measured = 15−290. Lines represent model prediction by eq 7.

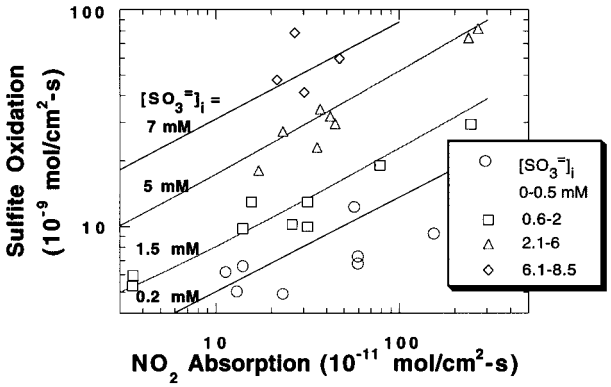

FIGURE 2. Model prediction of sulfite oxidation, pH = 5−7, 15% O_2, $Y_{NO_2,i}$ = 30−350 ppm.

The results with added Fe^{2+} and EDTA show that Fe^{2+} is an insignificant catalyst of sulfite oxidation in the presence of NO_2, although it can have a significant effect at lower rates of oxidation in the absence of NO_2. EDTA (0.02 mM) was added in several experiments to eliminate the effect of Fe^{2+} impurities (typically 0.005 mM in 0.3 M Na_2SO_4 solutions).

Effect of Thiosulfate on Sulfite Oxidation. In previous sections, we have shown the effect of thiosulfate on NO_2 absorption into sulfite solutions. Thiosulfate, as a free radical scavenger, is expected to play a more significant role in sulfite oxidation by providing an alternative route for the termination of a free radical reaction mechanism.

The free radical mechanism is initiated by the reaction between SO_3^{2-} and NO_2 (reaction 1), and the rate of initiation is given by eq 1, with $k_{2,SO_3^{2-}} = 11.2 \times 10^5$ M^{-1} s^{-1} at 55 °C.

The termination step of the mechanism is the reaction between $S_2O_3^{2-}$ and a free radical R• (eq 11), and the rate of termination is

$$r_t = k_t[S_2O_3^{2-}][R^\bullet] \tag{17}$$

Assuming the rate of initiation equals to the rate of termination, the steady-state concentration of $R^\bullet$ is

$$[R^\bullet] = \frac{k_{2,SO_3^{2-}}}{k_t}\frac{[NO_2][SO_3^{2-}]}{[S_2O_3^{2-}]} \tag{18}$$

The rate of oxidation is the rate of reaction between R• and

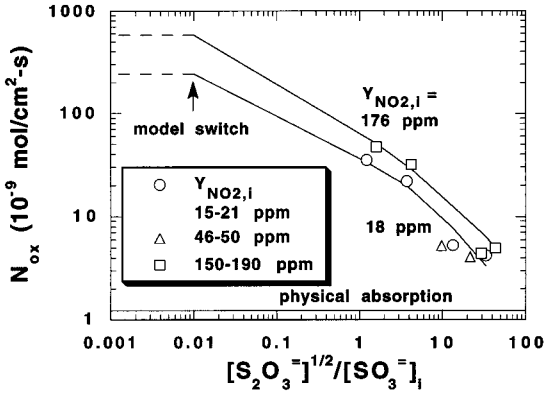

FIGURE 3. Model prediction of sulfite oxidation in the presence of thiosulfate, pH = 5.5 and 7.5, $[SO_3^{2-}]_i$ = 7−90 mM, 55 °C, 15% O_2.

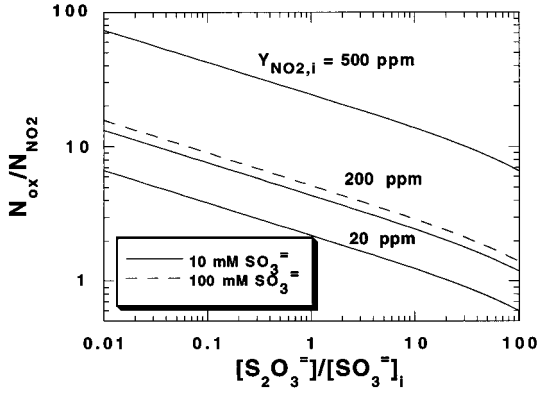

FIGURE 4. Calculated effect of NO_2 and SO_3^{2-} concentration on sulfite oxidation with $S_2O_3^{2-}$, pH > 7.5, 15% O_2, 55 °C.

SO_3^{2-}:

$$r_{ox} = k_{ox}[R^{\bullet}][SO_3^{2-}] \quad (19)$$

Substituting the expression for [R•] from eq 18 into eq 19, we have

$$r_{ox} = \frac{k_{ox}k_{2,SO_3^{2-}}}{k_t}\frac{[SO_3^{2-}]^2[NO_2]}{[S_2O_3^{2-}]} \quad (20)$$

The differential mass balance is

$$-D_{O_2}\frac{d^2[O_2]}{dx^2} = r_{ox} \quad (21)$$

To simplify the calculation, r_{ox} was assumed to be constant over the entire film thickness δ. Equation 21 was integrated over the entire thickness of δ, with the following boundary conditions:

$$@\ x = 0,\ [O_2] = [O_2]_i \text{ and } O_2 \text{ flux} = N_{ox}$$

$$@\ x = \delta,\ [O_2] = 0$$

Finally we have

$$N_{ox} = \sqrt{2D_{O_2}[O_2]_1\frac{k_{ox}k_{2,SO_3^{2-}}}{k_t}\frac{[SO_3^{2-}]_i^2[NO_2]_i}{[S_2O_3^{2-}]}} \quad (22)$$

where D_{O_2} is the diffusivity of O_2, with a value of 4.79×10^{-5} cm^2 s^{-1} at 55 °C, and N_{ox} is the measured rate of sulfite oxidation. A set of 10 experiments from Table 2 with varying concentrations of $[SO_3^{2-}]_i$, $[NO_2]_i$, and $[S_2O_3^{2-}]$ were used to regress the ratio of k_{ox} to k_t. At 55 °C, only experiments with thiosulfate at normal conditions were included. The regressed ratio is

$$\frac{k_{ox}}{k_t} = 3.43$$

Owens (*23*) reported a value of 4 for the above ratio at 50 °C.

Figure 3 gives the calculated rate of sulfite oxidation as a function of thiosulfate. The rate of sulfite oxidation decreases with increasing ratio of the square root of $[S_2O_3^{2-}]$ to $[SO_3^{2-}]_i$ but increases with $Y_{NO_2,i}$. An order of magnitude increase in the concentration of interfacial NO_2 leads to a factor of 3 increase in N_{ox}, consistent with the expression in eq 16. Furthermore, even with $([S_2O_3^{2-}]^{1/2}/[SO_3^{2-}]_i$ of 40, the rate of sulfite oxidation was still 3−4 times higher than that of physical absorption, indicating that sulfite oxidation is unavoidable with NO_2 absorption, even with the addition of thiosulfate. Noticeable deviation from the model is observed in two runs with 46−50 ppm $NO_{2,i}$. This is due to the fact that the solution pH for these two runs was around 5.5. At this pH, the oxidation of HSO_3^- started to become significant (*23*). All other runs in Figure 3 had pH > 7.5.

Figure 3 also shows the continuity between our model of sulfite oxidation without thiosulfate (eq 16) and the model of sulfite oxidation in the presence of thiosulfate (eq 22). When $([S_2O_3^{2-}])^{1/2}/[SO_3^{2-}]_i$ is greater than 0.01, the rate of sulfite oxidation can be predicted from eq 22. When $([S_2O_3^{2-}])^{1/2}/[SO_3^{2-}]_i$ is less than 0.01, eq 16 should be used to predict the rate of sulfite oxidation. The curves representing the two models intersected at $([S_2O_3^{2-}])^{1/2}/[SO_3^{2-}]_i$ = 0.01 for both NO_2 concentrations shown in Figure 3.

It has also become possible to estimate the number of moles of S(IV) oxidized for every mole of NO_2 absorbed in the presence of thiosulfate. The ratio of moles S(IV) oxidized to moles NO_2 absorbed can be expressed as the ratio of the rate of sulfite oxidation to the rate of NO_2 absorption, which is

$$\frac{N_{ox}}{N_{NO_2}} = \frac{\sqrt{2D_{O_2}[O_2]_i\frac{k_{ox}k_{2,SO_3^{2-}}}{k_t}\frac{[SO_3^{2-}]_i^2[NO_2]_i}{[S_2O_3^{2-}]}}}{\frac{P_{NO_{2,i}}}{H_{NO_2}}\sqrt{D_{NO_2}(k_{2,SO_3^{2-}}[SO_3^{2-}]_i + k_{2,S_2O_3^{2-}}[S_2O_3^{2-}]_i)}} \quad (23)$$

Figure 4 gives the above ratio as a function of $([S_2O_3^{2-}])^{1/2}/[SO_3^{2-}]_i$ at several interfacial NO_2 concentrations. The ratio of oxidation to NO_2 absorption decreases with increasing $([S_2O_3^{2-}])^{1/2}/[SO_3^{2-}]_i$ and decreasing NO_2 concentration, and it is not a strong function of $[SO_3^{2-}]_i$.

Results of Batch Experiments. A series of experiments were performed by operating the stirred-cell contactor in batch mode. The results of these experiments are summarized in Table 4. The second-order reaction rate constant (k_2) is given for the reaction between NO_2 and the primary reagent. Each of the experiments included a series of measurements with 200−1000 ppm NO_2. The absorbent concentrations given in Table 4 were not determined by solution analysis. They are either the nominal concentrations as prepared gravimetrically from reagent chemicals or the nominal concentration corrected for expected sulfite oxidation. Most of these experiments were performed at 25 °C and without O_2, so they are not directly comparable to the continuous experiments at 55 °C and in the presence of O_2.

Figure 5 gives NO_2 absorption as a function of $P_{NO_2,i}$ with 0.085−0.1 M reagents. The fastest rate of NO_2 absorption occurred in solutions of sulfite, indicating that it is the most effective reagent. On the other hand, NO_2 absorption in

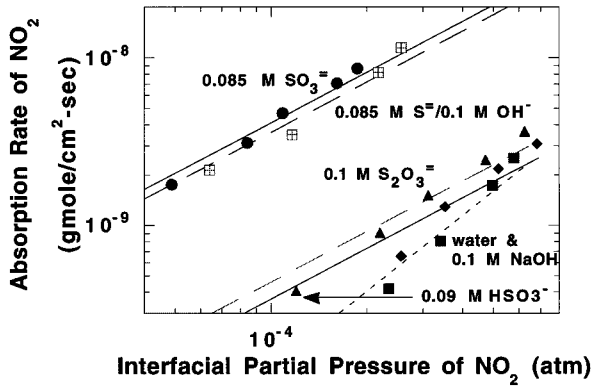

FIGURE 5. NO_2 absorption batch experiments, 25 °C, no O_2.

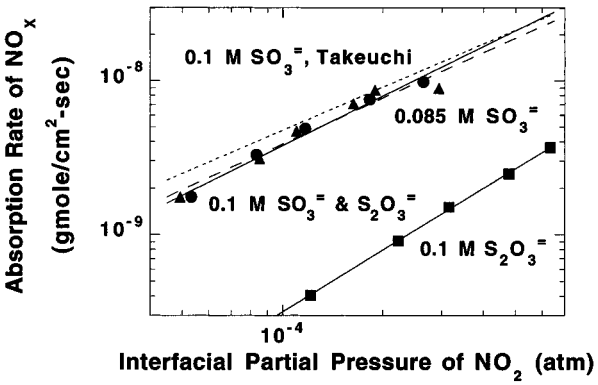

FIGURE 6. NO_2 absorption into sulfite, thiosulfate, and mixture at 25 °C.

thiosulfate or bisulfite solution is only slightly greater than in pure water. This trend was also observed by Takeuchi et al. (*5*).

Several of the batch experiments were intended to clarify the effect of O_2 on NO_2 absorption. The addition of 15% O_2 to the gas stream reduces NO_2 absorption in 0.1 M Na_2SO_3 solution by a factor of 2. However, the addition of $Na_2S_2O_3$ eliminates this effect, as shown in Figure 6. This is the same observation we have made with our continuous experiments. Takeuchi et al. (*22*) also reduced the oxidation effect with other inhibitors.

Industrial Implications. With the reaction rate constants between sulfite and NO_2, we can predict the NO_2 removal in a typical limestone slurry scrubber by:

$$\frac{1}{\ln\dfrac{Y_{NO_{2,in}}}{Y_{NO_{2,out}}}} = \frac{1}{N_g} + \frac{GH_{NO_2}}{A\sqrt{k_1 D_{NO_2}}} \qquad (24)$$

In eq 24, Y_{NO_2} is the mole fraction of NO_2, A is the gas−liquid contact area, and G is the gas flow rate. N_g, the number of gas film transfer units, was taken to be 6.9, typical of limestone slurry scrubbing (*27*). The ratio A/G was taken to be 2×10^5 atm cm^{-2} s^{-1} mol^{-1}. The effective first-order rate constant is given by

$$k_1 = k_{2,SO_3^{2-}}[SO_3^{2-}]_i + k_{2,HSO_3^-}[HSO_3^-] + \frac{2k_{2,H_2O}P_{NO_{2,i}}}{3H_{NO_2}} \qquad (25)$$

Figure 7 plots the fractional penetration of NO_2 as a function of interfacial S(IV) concentration in a typical scrubber. With typical conditions for limestone slurry, 10 mM total dissolved S(IV) and pH 4−5, the estimated NO_2 removal is less than 50%. Therefore, an acceptable level of

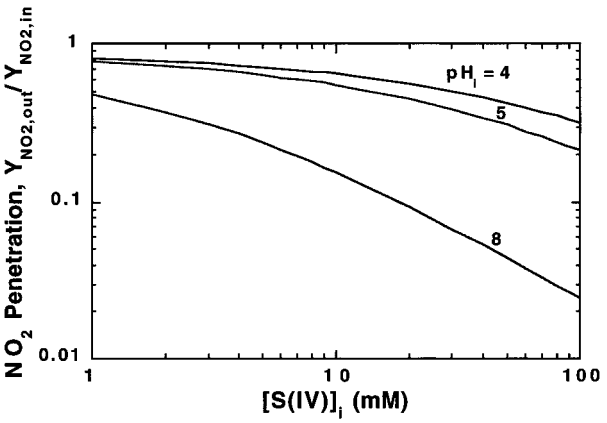

FIGURE 7. NO_2 removal in a typical limestone slurry scrubber. $N_g = 6.9$, $k_g = 3.4 \times 10^{-5}$ mol cm^{-2} s^{-1} atm^{-1}. Difference between solid and dotted line reflects the effect of NO_2 concentration on fraction NO_2 removal.

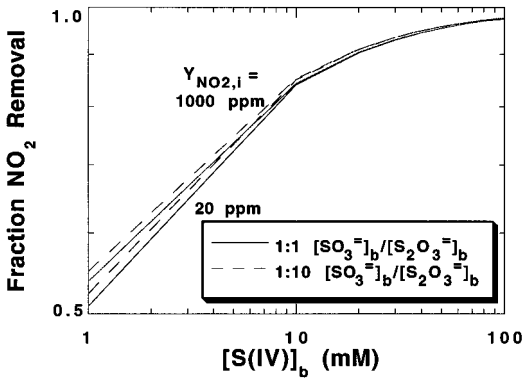

FIGURE 8. NO_2 removal in an aqueous Na_2SO_3 scrubber. $N_g = 6.9$, $k_g = 3.4 \times 10^{-5}$ mol cm^{-2} s^{-1} atm^{-1}, pH > 7.5, 55 °C, 15% O_2.

NO_2 removal by a conventional limestone slurry scrubber is not probable. Marginally acceptable performance might be possible in a forced oxidation system promoted by organic acids and by magnesium or sodium sulfate and controlled at the maximum level of dissolved sulfite.

However, our study also shows that Na_2SO_3 scrubbing, with the addition of $Na_2S_2O_3$ at high pH, is capable of achieving 95% NO_2 removal as shown in Figure 8. At pH 7.5, 80 mM or more total dissolved sulfite and at least a molar ratio of 1:1 thiosulfate sulfite are necessary for 95% removal of NO_2. Increasing the ratio of thiosulfate to sulfite does not lead to significant enhancement in NO_2 removal, but it would reduce the rate of sulfite oxidation and minimize the consumption of SO_3^{2-}.

Our study of sulfite oxidation also shows that it may be feasible to reduce the liquid depth in the hold tank in limestone slurry scrubbing by the addition of NO_2. NO_2 can be mixed with air and sparged into the hold tank, and oxidation in the hold tank will increase, resulting in considerable reduction of required liquid depth in the tank. By assuming a liquid depth of 30 ft is required to absorb 50% of the oxygen in the inlet air via physical absorption, a calculation was performed by integrating the NO_2-enhanced rate of oxidation over the new depth of liquid required to achieve the same level of oxygen absorption.

The calculated results in Figure 9 show that a significant reduction in hold tank liquid depth can be achieved by injecting 1000 ppm NO_2 at the bottom of the hold tank. This represents 1 mol of NO_2 injected for every 100 mol of O_2 absorbed. This ratio of NO_2:O_2 absorbed was necessary because the NO_2 was rapidly consumed by reaction with sulfite and thus was only able to initiate oxidation in a small

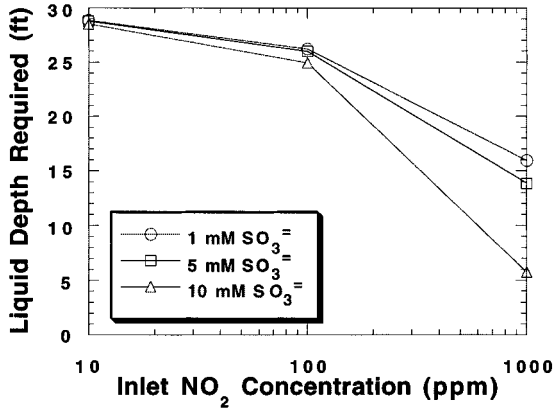

FIGURE 9. Reduction of hold tank liquid depth reduction by NO_2 injection. $Y_{O_2,in} = 0.2$, $Y_{O_2,out} = 0.1$. $A'/G = 1.9 \times 10^4$ cm s^{-1} mol^{-1}. NO_2 injection at bottom of tank, 55 °C.

segment of the liquid. An alternative method of NO_2 addition would be to inject smaller amounts of NO_2 at several different liquid depths. Since each injection of NO_2 would initiate sulfite oxidation over a small liquid depth, a lower concentration of NO_2 might be used.

Acknowledgments

This study has been supported by the Environmental Solutions Program of the University of Texas at Austin and by the United States Environmental Protection Agency.

Nomenclature

A	interfacial area, cm^2
C_1, C_2, C_3	regressed constants in sulfite oxidation model
D_{NO_2}	diffusion coefficient of NO_2, cm^2/s
D_{O_2}	diffusion coefficient of O_2, cm^2/s
G	gas flow rate, L/min
H_{NO_2}	Henry's constant of NO_2, cm^3 atm^{-1} mol^{-1}
$[HSO_3^-]_b$, $[HSO_3^-]_i$	bulk and interfacial concentration of HSO_3^-, M
k_{2,H_2O}	reaction rate constant for NO_2 and water, M^{-1} s^{-1}
k_{2,HSO_3^-}	reaction rate constant for NO_2 and bisulfite, M^{-1} s^{-1}
$k_{2,S_2O_3^{2-}}$	reaction rate constant for NO_2 and thiosulfate, M^{-1} s^{-1}
$k_{2,SO_3^{2-}}$, k_{ini}	reaction rate constant for NO_2 and sulfite, M^{-1} s^{-1}
k_g	gas-phase mass transfer coefficient, mol cm^{-2} s^{-1} atm^{-1}
k_l°	liquid-phase mass transfer coefficient, cm s^{-1}
k_{ox}	reaction rate constant for oxidation reaction, M^{-1} s^{-1}
k_t	reaction rate constant for termination step, M^{-1} s^{-1}
K_g	overall gas-phase mass transfer coefficient, mol cm^{-2} s^{-1} atm^{-1}
N_g	number of gas film transfer units
N_{NO_2}	flux of NO_2, mol cm^{-2} s^{-1}
N_{ox}	rate of sulfite oxidation, mol cm^{-2} s^{-1}
$[NO_2]_i$	interfacial concentration of NO_2, M
N_{SO_2}	rate of SO_2 absorption, mol cm^{-2} s^{-1}
$[O_2]_i$	interfacial O_2 concentration, M
$P_{NO_2,b}$, $P_{NO_2,i}$	bulk and interfacial partial pressure of NO_2, atm
r	rate of reaction, mol L^{-1} s^{-1}
R_g	normalized rate of NO_2 absorption, mol cm^{-2} s^{-1} atm^{-1}
$[SO_3^{2-}]_b$, $[SO_3^{2-}]_i$	bulk and interfacial concentration of SO_3^{2-}, M
$[SO_5^{\bullet-}]$	concentration of $SO_5^{\bullet-}$ radical, M
$[S(IV)]_o$, $[S(IV)]_f$	initial and final concentration of S(IV), M
$[S(IV)]_{tit}$	concentration of S(IV) in solution added to contactor, M
Δt	time interval, s
V	solution volume, L
V_{tit}	volume of solution added to contactor, mL
Y_{NO_2}	NO_2 mole fraction
$Y_{NO_2,b}$, $Y_{NO_2,i}$	bulk and interfacial concentration of NO_2, ppm
δ	film thickness, cm

Literature Cited

(1) Lyon, R. K.; Cole, J. A.; Kramlich, J. C.; Chen, S. L. *Combust. Flame* **1991**, *81*, 30.
(2) Izumi, J.; Murakami, N. U.S. Patent 4,350, 669, September 21, 1982.
(3) Borders, R. A.; Birks, J. W. *J. Phys. Chem.* **1982**, *86*, 3295.
(4) Baveja, K. K.; Rao, D. S.; Sarkar, M. K. *J. Chem. Eng. Jpn.* **1979**, *12*, 322−325.
(5) Takeuchi, H.; Ando, M.; Kizawa, N. *Ind. Eng. Chem., Process Des. Dev.* **1977**, *16*, 303.
(6) Takeuchi, H.; Yamanaka, Y. *Ind. Eng. Chem., Process Des. Dev.* **1978**, *17*, 389.
(7) Kameoka, Y.; Pigford, R. L. *Ind. Eng. Chem., Fundam.* **1977**, *16*, 163.
(8) Littlejohn, D.; Wang, Y.; Chang, S.-G. *Environ. Sci. Technol.* **1993**, *27*, 2161.
(9) Shen, C.; Rochelle, G. T. Nitrogen Dioxide Absorption and Sulfide Oxidation in Aqueous Sulfide. *J. Air Waste Manage. Assoc.* In press.
(10) Shen, C. Nitrogen Dioxide Absorption in Aqueous Sodium Sulfite. Ph.D. Dissertation, The University of Texas at Austin, May 1997.
(11) McGuire, L. M. Sulfur Dioxide Absorption Experiments in Calcium Hydroxide Slurries. M.S. Thesis, University of Texas at Austin, 1990.
(12) Tseng, C. H. P. Calcium Sulfite Hemihydrate Dissolution and Crystallization. Ph.D. Dissertation, University of Texas at Austin, 1984.
(13) Thorn, P. R., Jr. Diethlenetriamine Solutions for Stack Gas Desulfurization by Absorption/Stripping. M.S. Thesis, University of Texas at Austin, 1981.
(14) Nash, T. *Atmos. Environ.* **1979**, *13*, 1149.
(15) Danckwerts, P. V. Absorption into Agitated Liquids. In *Gas−Liquid Reactions*; McGraw-Hill: New York, 1970.
(16) Glasscock, D. A.; Rochelle, G. T. *AIChE J.* **1993**, *39*, 1389.
(17) Wilke, C. R.; Chang, P. *AIChE J.* **1955**, *1*, 261.
(18) Andrew, S. P. S.; Hanson, D. *AIChE J.* **1965**, *11*, 105.
(19) Oblath, S. B.; Markowitz, S. S.; Novakov, T.; Chang, S. G. *J. Phys. Chem.* **1982**, *86*, 4853.
(20) Oblath, S. B.; Markowitz, S. S.; Novakov, T.; Chang, S. G. *J. Phys. Chem.* **1981**, 85, 1017.
(21) Huie, R. E.; Neta, P. *J. Phys. Chem.* **1984**, *88*, 5665.
(22) Takeuchi, H.; Takahashi, K.; Kizawa, N. *Ind. Eng. Chem., Process Des. Dev.* **1977**, *16*, 486.

(23) Owens, D. R. Sulfite Oxidation Inhibited by Thiosulfate. M.S. Thesis, University of Texas at Austin, 1984.

(24) Epstein, M. *EPA Alkali Scrubbing Test Facility: Summary of Testing Through October 1974*. EPA-650/2-75-047; NTIS PB-244 901; U.S. Government Printing Office: Washington, DC, 1975.

(25) Clifton, C. L.; Altstein, N.; Huie, R. E. *Environ. Sci. Technol.* **1988**, *22*, 5586−589.

(26) Clarke, A. G.; Radojevic, M. *Atmos. Environ.* **1983**, *17*, 617.

(27) Agarwal, R. S. Limestone Slurry Scrubbing-Modeling and Parameter Estimation. Ph.D. Dissertation, University of Texas at Austin, 1995.

Received for review May 27, 1997. Revised manuscript received April 14, 1998. Accepted April 20, 1998.

ES970466Q